
FEW-SHOT INSPIRED GENERATIVE ZERO-SHOT LEARNING

Md Shakil Ahamed Shohag

Department of Electrical and Computer Engineering
University of Windsor
Canada
shakilshohag@gmail.com

Q. M. Jonathan Wu

Department of Electrical and Computer Engineering
University of Windsor
Canada
jwu@uwindson.ca

Farhad Pourpanah

Department of Electrical and Computer Engineering
Queen's University
Canada
farhad.086@gmail.com

ABSTRACT

Generative zero-shot learning (ZSL) methods typically synthesize visual features for unseen classes using predefined semantic attributes, followed by training a fully supervised classification model. While effective, these methods require substantial computational resources and extensive synthetic data, thereby relaxing the original ZSL assumptions. In this paper, we propose FSIGenZ, a few-shot-inspired generative ZSL framework that reduces reliance on large-scale feature synthesis. Our key insight is that class-level attributes exhibit instance-level variability, i.e., some attributes may be absent or partially visible, yet conventional ZSL methods treat them as uniformly present. To address this, we introduce Model-Specific Attribute Scoring (MSAS), which dynamically re-scores class attributes based on model-specific optimization to approximate instance-level variability without access to unseen data. We further estimate group-level prototypes as clusters of instances based on MSAS-adjusted attribute scores, which serve as representative synthetic features for each unseen class. To mitigate the resulting data imbalance, we introduce a Dual-Purpose Semantic Regularization (DPSR) strategy while training a semantic-aware contrastive classifier (SCC) using these prototypes. Experiments on SUN, AwA2, and CUB benchmarks demonstrate that FSIGenZ achieves competitive performance using far fewer synthetic features.

Keywords Zero-shot learning · generalized zero-shot learning · knowledge transfer · contrastive learning · feature synthesis

1 Introduction

Zero-shot learning (ZSL) aims to recognize unseen classes by transferring knowledge from seen classes using semantic information, such as attributes or word vectors [1, 2]. This is crucial for tasks where collecting labeled data for every class is impractical. ZSL methods can be categorized by classification range: (i) conventional ZSL (CZSL), which predicts only unseen classes, and (ii) generalized ZSL (GZSL), which considers both seen and unseen classes during inference [3].

Early ZSL methods focus on learning a shared embedding space that maps visual features of seen classes to their corresponding semantic representations, enabling classification via similarity-based matching [2]. Although effective in transferring knowledge, these embedding-based methods often exhibit a strong bias toward seen classes in the GZSL setting, which leads to misclassifications of unseen instances [4]. To mitigate this bias, generative approaches leverage models such as generative adversarial networks (GANs) [5] and variational autoencoders (VAEs) [6] to synthesize visual features for unseen classes using semantic and visual information from seen classes. This strategy transforms ZSL into a fully supervised learning task and reduces the seen-class bias [7]. However, existing generative methods

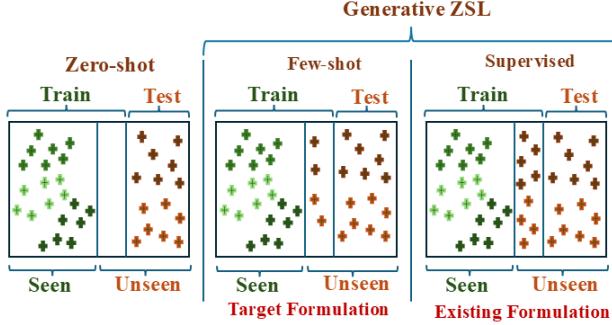


Figure 1: Conceptual illustration: FSL is a less relaxed problem formulation of ZSL than the supervised formulation.

often synthesize a large volume of features without assessing their actual utility for classification [8]. Moreover, this large-scale feature generation represents a highly relaxed ZSL setting and overlooks more constrained and realistic scenarios, such as few-shot learning (FSL), where only a limited number of examples per unseen class are available (see Fig. 1).

In our analysis, we found that many images exhibit missing or partially present attributes (see Fig. 2(a)). For example, while 'Furry' is consistently present, attributes such as 'Quadrupedal,' 'Tail,' and 'Hooves' are absent or only partially visible. This instance-level variability is overlooked by class-level semantics. Based on this observation, we propose two key insights: (i) attribute scores should be dynamic to reflect the degree of presence in individual instances, and (ii) instances can be meaningfully grouped based on these attribute scores (see Fig. 2(b)). However, implementing instance-level attribute scoring is challenging in ZSL as unseen classes lack instance-level data during training, making it impossible to capture attribute variations directly.

To overcome this, we propose *Model-Specific Attribute Scoring (MSAS)* (Section 3.3), which re-scores class-level attributes to model-optimized values by treating them as hyperparameters. This enables the model to better align with the true attribute variability without requiring access to unseen class instances. Building on MSAS, we estimate centroids of these attribute-based groups (Fig. 2(b)) to serve as prototypes for each unseen class. These group-level prototypes act as representative instances during training and eliminate the need for large-scale feature generation that helps reduce computational overhead. To further address the class imbalance caused by this reduced feature synthesis, we employ a semantic-aware contrastive classifier (SCC), which leverages visual-semantic contrastive learning coupled with a semantic regularization strategy to enhance class discrimination and semantic alignment. Extensive experiments on three benchmark datasets (**SUN** [9], **AwA2** [1], and **CUB** [10]) demonstrate that our approach achieves performance comparable to state-of-the-art methods while using substantially fewer synthetic features.

The key contributions of this study include: (i) We reformulate generative ZSL by drawing inspiration from FSL, shifting away from the conventional fully supervised paradigm, (ii) We propose a unified generative ZSL framework that synthesizes a limited set of group-level prototypes for unseen classes and addresses data imbalance using a semantic-aware contrastive classifier, and (iii) We conduct comprehensive experiments and ablation studies on multiple benchmark datasets to validate the effectiveness and robustness of the proposed method.

2 Related Works

Embedding methods retain the original training dataset and use samples from seen classes to learn a classifier that generalizes to unseen classes. These methods differ primarily in the space where classification is performed—visual, semantic, or a shared latent embedding space [3]. Visual embedding learns a projection from attributes to visual space, either by mapping semantic attributes into visual prototypes [11] or by leveraging semantic relationships between classes to build a classifier for unseen classes [12, 13]. Semantic embedding maps visual features into the semantic space [14], while latent embedding maps both visual and semantic spaces into a shared latent space to bridge seen and unseen class gaps [15].

Generative methods use seen class images and semantic information of both seen and unseen classes to synthesize visual features for unseen classes, which are then used to train classifiers for ZSL tasks. A key approach is GANs conditioned on unseen class semantics, such as f-CLSWGAN [7], which generates visual features for unseen categories and matches them to semantic attributes in a joint embedding space. f-VAEGAN [16] combines VAEs and GANs into a unified framework, while FREE [17] enhances features within this framework to mitigate cross-dataset bias. ZeroGen [18] leverages pre-trained language models to synthesize datasets for zero-shot tasks. Recent works integrate

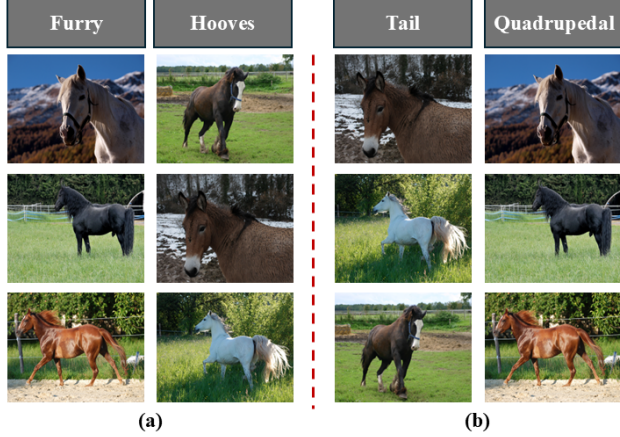


Figure 2: Our observations: Even for four attributes—Furry, Hooves, Tail, and Quadrupedal—(a) shows ungrouped instances of the horses as if they share identical attribute scores, while (b) conceptualizes how instances can be grouped (each row) based on varying degrees of attribute presence or absence.

embedding models with feature generation models to boost recognition across seen and unseen classes [19–21], such as CE-GZSL [19], which incorporates contrastive embedding with class- and instance-level supervision, and RE-GZSL [20], which extrapolates unseen class features using semantic relations with seen classes, contrastive losses, and a feature mixing module for more realistic and discriminative samples.

However, GAN-based generative methods often face challenges such as high computational costs [22] and mode collapse [23], and they do not inherently structure data representations in ways that are intuitive or easy to integrate with other models [8]. Alternatively, several methods [24–29] synthesize samples without adversarial training. For example, methods like Composer [26] and ABS-Net [27] extract and combine attribute-based features to create pseudo samples for unseen classes, while BPL [28] and AGZSL [29] use interpolation and perturbation to transfer class-specific variations from seen to unseen classes. Our approach aligns with these methods and synthesizes feature cluster centers of unseen classes as training data following a non-adversarial strategy.

3 Approach

3.1 Problem Settings

In ZSL, there are K seen classes (\mathcal{Y}^s) and L unseen classes (\mathcal{Y}^u), with $\mathcal{Y}^s \cap \mathcal{Y}^u = \emptyset$. Indices $\{1, \dots, K\}$ correspond to seen classes, and $\{K + 1, \dots, K + L\}$ to unseen classes. The seen data comprises N labeled images represented as $D = \{(\mathbf{x}_i, y_i) | \mathbf{x}_i \in \mathcal{X}, y_i \in \mathcal{Y}^s\}_{i=1}^N$, while labeled samples for unseen classes are unavailable. The visual sample space is \mathcal{X} , and class-wise semantic attributes $\mathbf{A}_o = \{\mathbf{a}_c\}_{c=1}^{K+L}$ link seen and unseen classes. The goal in CZSL is to learn a classifier mapping $\mathcal{X} \rightarrow \mathcal{Y}^u$, while GZSL aims for $\mathcal{X} \rightarrow \mathcal{Y}^s \cup \mathcal{Y}^u$.

3.2 Model Overview

Fig. 3 presents FSIGenZ, a unified zero-shot learning framework that seamlessly integrates feature generation and contrastive classification. In phase 1, it utilizes the MSAS scheme to re-score attributes and then estimates a compact yet semantically diverse set of subgroup prototypes per unseen class which capture intra-class variability without requiring unseen data. Instead of large-scale feature generation, these prototypes are included as synthetic training data for unseen classes. In phase 2, FSIGenZ employs the SCC unit built on visual-semantic contrastive learning along with a semantic regularization technique to address unseen class imbalance caused by limited feature generation. The complete process is detailed in Algorithm 1, with each component elaborated in subsequent sections.

3.3 Model-Specific Attribute Scoring (MSAS)

In general, attributes describe classes as a whole, and specifying them for individual instances is impractical. *MSAS* balances between this impracticality and the need for instance-level specifications of attributes by tailoring them toward the model’s requirements. While one might treat each attribute as a hyperparameter, the brute-force approach of tuning

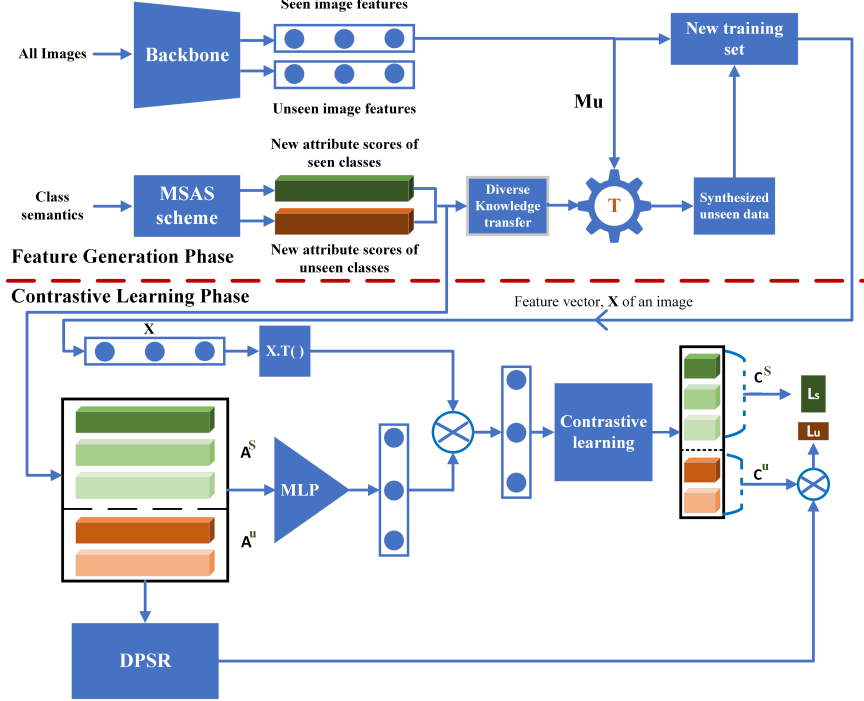


Figure 3: Overview of the FSIGenZ framework. The model comprises two main phases: feature generation (above the red dotted line) and contrastive learning (below). Symbols \otimes and ‘T’ represent element-wise multiplication and semantic knowledge transfer, respectively. Green-toned elements denote seen classes, while orange-toned elements denote unseen classes.

every attribute as a hyperparameter is infeasible. Instead, MSAS redetermines attribute scores using collective measures such as thresholding and reweighting, which enable the model to utilize the most appropriate attribute values. In this paper, we employ a straightforward equation for MSAS:

$$\mathbf{A} = (\mathbf{A}_o + \mathbf{A}_{mdf})W_A, \quad (1)$$

where W_A is a weight scalar, \mathbf{A}_o is the original attribute matrix, and \mathbf{A}_{mdf} is defined as:

$$\mathbf{A}_{mdf} = \mathbf{A}_o \odot (\mathbf{A}_o > T_h), \quad (2)$$

where \odot denotes element-wise multiplication, and $(\mathbf{A}_o > T_h)$ is an indicator function producing a binary mask (1 if true, 0 otherwise). Adjusting hyperparameters W_A and T_h allows the model to align attribute scores with the optimal configuration.

3.4 Unseen Data Synthesis

Unlike conventional generative ZSL methods, our approach estimates subgroup prototypes of instances within each unseen class by modeling instance-level variations of attributes. These prototypes are then utilized as representative training samples. Inspired by MDP [30], we employ a multi-source knowledge transfer strategy to synthesize data for unseen classes by transferring the semantic embedding manifold into the visual feature space. To begin, we estimate virtual class centers for unseen classes using:

$$A^u = R_s(A^s) \Rightarrow M^u = R_s(M^s), \quad (3)$$

where A^u and A^s denote the attribute vectors for unseen and seen classes, respectively, M^u and M^s represent the mean cluster centers for unseen and seen classes, and R_s is the relation function mapping seen classes to unseen classes.

In this formulation, the attribute embeddings A^u of unseen classes are estimated by applying the relation function R_s to the seen class attributes A^s . Subsequently, virtual class centers M^u for unseen classes are obtained by applying R_s to the cluster centers M^s of seen classes. The relation function $R_s(\cdot)$ is learned through Sparse Coding, as:

$$\min_{\alpha} \|a_c^u - A^s \alpha\|_2^2 + \lambda \|\alpha\|_2^2, \quad (4)$$

Algorithm 1: FSIGenZ

Input: Images I , class attributes \mathbf{A}_o , initialization Θ^0
Output: ZSL classifier

- 1: *# Extract Features*
- 2: **for** each image i **do**
- 3: Extract ViT features: $F_i^{S+U} \leftarrow \text{ViT}(I_i)$
- 4: **end for**
- 5: Apply MSAS on class attributes: $\mathbf{A} \leftarrow \mathbf{A}_o$
- 6: *# Synthesize Unseen Features*
- 7: Compute relation matrices, $\alpha_p \leftarrow R_{s_p}$ for different λ_p values
- 8: Estimate group clusters for unseen classes: $\mu_{k_p}^u \leftarrow M_s \alpha_p$
- 9: Utilize $\mu_{k_p}^u$ as synthetic unseen features
- 10: Obtain augmented train data, F by combining synthetic unseen data and real train data
- 11: *# Train the Semantic-Aware Contrastive Classifier (SCC)*
- 12: **for** each iteration t **do**
- 13: Encode class semantics with MLP: $E_j \leftarrow \text{MLP}(\mathbf{a}_j)$
- 14: Fuse features: $Z_{ij} \leftarrow F_i \otimes E_j$
- 15: Compute class scores: $c_{ij} \leftarrow f(Z_{ij})$
- 16: Apply Dual-Purpose Semantic Regularization (DPSR)
- 17: **end for**
- 18: *# Perform Inference*
- 19: **for** a given test image i **do**
- 20: Predict CZSL class: $y_i^{CZSL} \leftarrow \arg \max_j \{c_{ij}\}_{j=K+1}^{K+L}$
- 21: Predict GZSL class: $y_i^{GZSL} \leftarrow \arg \max_j \{c_{ij}\}_{j=1}^{K+L}$
- 22: **end for**

where $\alpha = [\alpha_1, \dots, \alpha_K]^T$ is the sparse coefficient vector, and λ is the regularization parameter.

Finally, the estimated cluster center μ_k^u of the k^{th} unseen classes is obtained as:

$$\mu_k^u = M^s \alpha, \quad (5)$$

where μ_k^u represents the estimated cluster center of the k^{th} unseen class.

While estimating a single cluster center per unseen class is relatively straightforward, the challenge arises when multiple centers must be calculated for each class. Addressing this complexity requires a solid theoretical foundation. Our observations, illustrated in Fig. 2, offer crucial insights to support this approach.

Our method leverages dynamic attribute scores through two key mechanisms. The first involves our MSAS strategy (Sec.3.3), and the second builds on the idea of inducing variation by adjusting the regularization parameter λ in equation (4), which in turn generates different sparse coefficient vectors α . Substituting these diverse α values into equation (5) results in multiple cluster centers per unseen class. These centers act as visual prototypes, each capturing a subset of instances that share similar semantic traits, as shown in Fig. 2(b).

In our few-shot-inspired setup, this process of tuning λ yields distinct advantages. It leads to varied, sparse representations that reflect meaningful subgroups within each class. By modeling dominant attribute combinations, the resulting prototypes represent intra-class diversity in a compact and informative manner. Importantly, this approach introduces minimal computational overhead, as only a limited number of prototypes are generated. In essence, the controlled variation of λ offers an efficient and principled way to simulate the natural heterogeneity found within unseen classes—an idea that aligns with and supports the core design of FSIGenZ.

3.5 Semantic-Aware Contrastive Classifier (SCC)

The Semantic-Aware Contrastive Classifier (SCC) begins by augmenting synthesized features of unseen classes with real features from seen classes, forming a unified training set. Let $F(\mathbf{x}_i)$ denote the feature representation of the i^{th} instance, and $E(\mathbf{a}_j)$ represent the embedding of the semantic descriptor for class j . The fused feature Z_{ij} is computed via a fusion operation, such as element-wise multiplication:

$$Z_{ij} = F(\mathbf{x}_i) \otimes E(\mathbf{a}_j). \quad (6)$$

To measure the compatibility between instance i and class j , we define a contrastive score c_{ij} , computed as:

$$c_{ij} = f(Z_{ij}), \quad (7)$$

where f is a contrastive learning function.

Next, we formulate a one-hot class indicator vector m_{ij} , based on the ground-truth class label y_i of instance i :

$$m_{ij} = \begin{cases} 1, & \text{if } y_i = j \\ 0, & \text{if } y_i \neq j \end{cases}. \quad (8)$$

Using these definitions, we can train a classifier to learn visual-semantic alignment by minimizing the following contrastive loss over the unified dataset, which contains both real and synthetic samples:

$$\mathcal{L}_{\mathcal{N}} = - \sum_{i=1}^{N+N^S} \sum_{j=1}^{K+L} m_{ij} \log(c_{ij}) + (1 - m_{ij}) \log(1 - c_{ij}), \quad (9)$$

where N^S is the number of synthesized features for unseen classes.

However, this formulation does not account for class imbalance, particularly among the unseen classes, where only a small number of synthetic instances are generated, consistent with our few-shot-inspired ZSL framework. To address this challenge, we introduce a semantic regularization strategy in the following section.

Training Strategy: To formulate the training objective, we partition the class indicator m_{ij} and the contrastive score c_{ij} into seen and unseen class components, denoted by superscript S and U, respectively. For each training sample, whether real (from seen classes) or synthetic (from unseen classes), we compute two separate losses. The first loss, $\mathcal{L}_{\mathcal{S}}$, is a binary cross-entropy (BCE) loss applied to the model's predictions over seen classes:

$$\mathcal{L}_{\mathcal{S}} = - \sum_{i=1}^{N+N^S} \sum_{j=1}^K m_{ij}^s \log(c_{ij}^s) + (1 - m_{ij}^s) \log(1 - c_{ij}^s), \quad (10)$$

Given that synthetic features are generated from a limited set of group prototypes, they may not fully reflect the complexity of real data. To mitigate this, we introduce a semantically regularized BCE loss $\mathcal{L}_{\mathcal{U}}$, which operates on the model's predictions over unseen classes. This loss incorporates a semantic similarity mask s_{ij}^u , which encodes the relationship between the ground-truth class and all other unseen classes. The formulation is:

$$\mathcal{L}_{\mathcal{U}} = - \sum_{i=1}^{N+N^S} \sum_{j=K+1}^L m_{ij}^u \log(c_{ij}^u s_{ij}^u) + (1 - m_{ij}^u) \log(1 - c_{ij}^u s_{ij}^u), \quad (11)$$

where s_{ij}^u is a regularization term obtained by the Dual-Purpose Semantic Regularization (DPSR) module, discussed below. The total training loss combines these components:

$$\mathcal{L} = \mathcal{L}_{\mathcal{S}} + \beta \mathcal{L}_{\mathcal{U}}, \quad (12)$$

where β is a hyperparameter that controls the contribution of the regularized unseen-class loss.

Dual-Purpose Semantic Regularization (DPSR): A key challenge in our ZSL formulation is the imbalance between seen data and synthetic unseen data. This disparity may lead the classifier to form overly confident decision boundaries for seen classes, while producing uncertain or unreliable predictions for unseen ones. To address this issue, we propose DPSR, a regularization strategy that enhances classifier training by incorporating semantic relationships between classes. The core idea is to guide the model using class-to-class semantic similarities. These similarities are obtained by solving the following optimization problem:

$$s_p = \arg \min_{s_p} \left\| \mathbf{a}_p - \sum_{q=1}^{K+L} \mathbf{a}_q s_{pq} \right\|_2^2 + \phi \|s_p\|_2, \quad (13)$$

where \mathbf{a}_p represents the semantic embedding of class p , and s_{pq} is the q^{th} element of the similarity vector s_p , representing the semantic proximity between class p and class q . The regularization parameter ϕ prevents trivial solutions by discouraging any single similarity score, particularly self-similarity, from dominating. Once the similarity vector is obtained, it is normalized to form a probability-like distribution:

$$s_{pq} = \frac{s_{pq}}{\sum_{q=1}^{K+L} s_{pq}}. \quad (14)$$

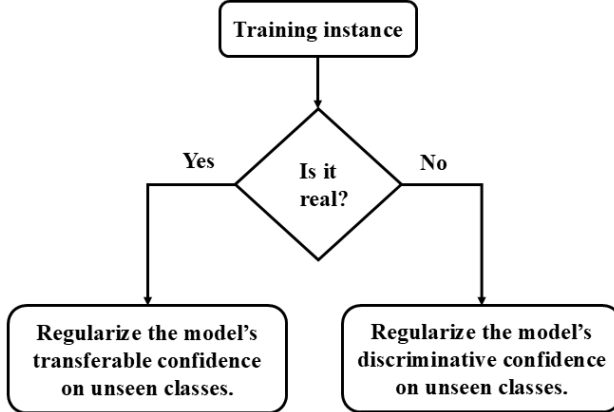


Figure 4: DPSR conceptualized in a flowchart: regularization of model’s transferable and discriminative confidence to improve unseen class generalization.

This ensures that similarity scores across all classes are scaled appropriately

For any class p , the semantic similarity to any unseen class q is denoted as s_{pq}^u , and is drawn from the computed vector s_p . These similarity values are used to modulate the model’s predictions for unseen classes within the contrastive loss function. In doing so, DPSR helps guide learning toward decision boundaries that are more consistent with the underlying semantic structure.

DPSR tackles the challenge of data imbalance in unseen classes using a twofold strategy. First, for every training instance, the model generates prediction scores across both seen and unseen classes. For training instances belonging to seen classes, DPSR adjusts the transferable scores assigned to unseen classes by encouraging alignment with their semantic similarity to the true class. This helps promote reasonable activations for semantically related unseen classes while suppressing unrelated ones. Unlike existing approaches that adjust unseen scores post hoc [31–33], this adjustment is integrated directly into the training process through semantic regularization. Second, for synthetic unseen instances, DPSR softens the discriminative loss signal among unseen classes to enhance robustness and generalization in the low-data regime. This regularization improves generalization by preventing the model from drawing overly sharp decision boundaries based on limited or imprecise data. Altogether, DPSR helps the classifier make more stable and semantically grounded predictions for unseen classes (see Fig. 4). It is worth noting that DPSR is used exclusively during training; at inference, the model outputs raw predictions without any regularization.

3.6 Zero-Shot Recognition

We perform zero-shot recognition by computing contrastive scores between the visual representation of an input and the semantic embedding of all classes. In the CZSL, the prediction is restricted to unseen classes, and an input image is assigned to the class with the highest contrastive score among them:

$$\mathcal{P}_{czsl}(x_i) = \max_j \{c_{ij}\}_{j=K+1}^{K+L}. \quad (15)$$

In the GZSL setting, predictions are made over both seen and unseen classes. Accordingly, the image is assigned to the class (either seen or unseen) with the highest contrastive score:

$$\mathcal{P}_{gzsl}(x_i) = \max_j \{c_{ij}\}_{j=1}^{K+L}. \quad (16)$$

4 Experimental studies

This section presents the experimental setup, including the datasets, evaluation protocols, and implementation details. It then reports the experimental results and ablation studies.

4.1 Experimental Setup

Datasets. We evaluate our approach on three ZSL datasets: SUN [9], AwA2 [1], and CUB [10]. AwA2 is a medium-scale, coarse-grained dataset with 37,322 images from 50 animal categories, described by 85 attributes. CUB is a

Table 1: Results of methods on CZSL (T1) and GZSL (H) tasks. Overall best and second-best results are bolded and underlined, while red and blue highlight the best and second-best among generative methods, respectively.

Method	SUN				AwA2				CUB				
	T1	U	S	H	T1	U	S	H	T1	U	S	H	
Embedding-based	TCN [34]	61.5	31.2	37.3	34.0	71.2	61.2	65.8	63.4	59.5	52.6	52.0	52.3
	DAZLE [31]	-	52.3	24.3	33.2	-	60.3	75.7	67.1	65.9	56.7	59.6	58.1
	ViT-ZSL [35]	-	44.5	55.3	49.3	-	51.9	90.0	65.8	-	67.3	75.2	71.0
	MSDN [36]	65.8	52.2	34.2	41.3	70.1	62.0	74.5	67.7	76.1	68.7	67.5	68.1
	SCILM [37]	62.4	24.8	32.6	28.2	71.2	48.9	77.8	60.1	52.3	24.5	54.9	33.8
	DUET [4]	64.4	45.7	45.8	45.8	69.9	63.7	84.7	72.7	72.3	62.9	72.8	67.5
	BGSNet [38]	63.9	45.2	34.3	39.0	69.1	61.0	81.8	69.9	73.3	60.9	73.6	66.7
	PRZSL [39]	64.2	53.6	37.7	44.4	73.6	65.8	77.8	71.3	77.1	68.8	63.7	66.2
	ZS-VAT [40]	62.6	45.6	33.8	38.8	72.2	59.9	80.8	68.8	75.2	67.5	68.1	67.8
Generative-based	f-CLSWGAN [7]	60.8	42.6	36.6	39.4	-	-	-	-	57.3	43.7	57.7	49.7
	f-VAEGAN-D2 [16]	64.7	45.1	38.0	41.3	71.1	57.6	70.6	63.5	61.0	48.4	60.1	53.6
	OCD-CVAE [41]	63.5	44.8	42.9	43.8	71.3	59.5	73.4	65.7	60.3	44.8	59.9	51.3
	TF-VAEGAN [42]	<u>66.0</u>	45.6	40.7	43.0	72.2	59.8	75.1	66.6	64.9	52.8	64.7	58.1
	HSVA [43]	63.8	48.6	39.0	43.3	-	56.7	79.8	66.3	62.8	52.7	58.3	55.3
	TGMZ [44]	-	-	-	-	-	64.1	77.3	70.1	-	60.3	56.8	58.5
	GCM-CF [45]	-	47.9	37.8	42.2	-	60.4	75.1	67.0	-	61.0	59.7	60.3
	CE-GZSL [19]	63.3	48.8	38.6	43.1	70.4	63.1	78.64	70.0	77.5	63.9	66.8	65.3
	FREE [17]	-	47.4	37.2	41.7	-	60.4	75.4	67.1	-	55.7	59.9	57.7
	AGZSL [29]	63.3	29.9	40.2	34.3	73.8	65.1	78.9	71.3	57.2	41.4	49.7	45.2
	SE-GZSL [46]	-	45.8	40.7	43.1	-	59.9	80.7	68.8	-	53.1	60.3	56.4
	ICCE [21]	-	-	-	-	72.7	65.3	82.3	72.8	78.4	67.3	65.5	66.4
	TDCSS [24]	-	-	-	-	-	59.2	74.9	66.1	-	44.2	62.8	51.9
	LCR-GAN [47]	-	57.6	43.8	49.8	-	-	-	-	-	53.6	67.5	59.7
	DFCA-GZSL [48]	62.6	48.9	38.8	43.3	<u>74.7</u>	66.5	81.5	73.3	<u>80.0</u>	70.9	63.1	66.8
	RE-GZSL [20]	-	-	-	-	73.1	67.7	81.1	<u>73.8</u>	78.9	72.3	62.4	67.0
	AREES [49]	64.3	51.3	35.9	42.2	73.6	57.9	77.0	66.1	65.7	53.6	56.9	55.2
	JFGOPL [50]	-	48.8	38.0	42.7	-	62.6	74.2	67.9	-	56.4	62.7	59.4
	DENet [51]	-	52.3	40.8	45.8	-	62.6	84.8	72.0	-	65.0	71.9	68.3
	DPCN [52]	63.8	48.1	39.4	43.3	70.6	65.4	78.6	71.4	80.1	72.7	65.7	69.0
	Zheng et al. [53]	-	-	-	-	-	63.3	74.0	68.2	-	71.0	65.7	68.3
	FSIGenZ (Ours)	67.8	42.5	49.9	45.9	75.0	67.6	82.3	74.2	73.0	65.9	72.7	<u>69.1</u>

fine-grained dataset with 11,788 images from 200 bird species, each with 312 attributes. SUN is another fine-grained dataset, comprising 14,340 images across 717 scene types with 102 attributes.

Baselines. We evaluate the performance of our proposed method against a wide range of existing approaches, including several generative-based models. Specifically, we compare with TCN [34], DAZLE [31], ViT-ZSL [35], MSDN [36], SCILM [37], DUET [4], BGSNet [38], PRZSL [39], ZS-VAT [40], f-CLSWGAN [7], f-VAEGAN-D2 [16], OCD-CVAE [41], TF-VAEGAN [42], HSVA [43], TGMZ [44], GCM-CF [45], CE-GZSL [19], FREE [17], AGZSL [29], SE-GZSL [46], ICCE [21], TDCSS [24], LCR-GAN [47], DFCA-GZSL [48], RE-GZSL [20], AREES [49], JFGOPL [50], DENet [51] and DPCN [52]. By benchmarking against this wide range of models, we ensure a comprehensive evaluation of our method’s effectiveness in both ZSL settings.

Evaluation Protocols. We evaluate performance under CZSL and GZSL settings. In CZSL, we report the average per-class Top-1 accuracy (T1) on unseen classes. In GZSL, we compute Top-1 accuracies for seen (S) and unseen (U) classes, and use their harmonic mean $H = 2 \times \frac{S \times U}{S + U}$ to assess balanced performance across seen and unseen classes.

Implementation Details. We extracted 786-dimensional image features using the ViT-Base [54] backbone pre-trained on ImageNet-1k and used attributes provided in [1]. In MSAS, we set W_A and T_h as $\{0.005, 0.08, 0.3\}$ and $\{0.7, 0.8, 0.7\}$ for SUN, AwA2 and CUB, respectively. For the required number of feature generation per unseen class of a dataset, λ takes the same number of random values between 1 and 1.02. Our SCC unit is inspired by [34], with a modified structure tailored to integrate both our underlying theoretical foundation and synthetic features from unseen classes. Specifically, our architecture includes a two-layer fully connected network to transform class semantics with 1024 and 786 units in the first and second layers, respectively. Contrastive learning is performed with a separate fully connected network featuring a 1024-dimensional hidden layer and a single-dimensional output. ReLU and Leaky ReLU are used

Table 2: Unseen data statistics of different methods after including synthetic features. N^{USF} , N^{URF} , and N_P^{SF} denote number of unseen synthetic features, number of unseen real features and number of synthetic features per class, respectively. (U/S) indicates whether the synthetic features are generated exclusively for unseen classes or for both seen and unseen classes.

Method	SUN				AwA2				CUB				
	T1	H	N^{USF}	N^{URF}	T1	H	N^{USF}	N^{URF}	T1	H	N^{USF}	N^{URF}	N_P^{SF}
HSVA [43]	63.8	43.3	28800/14400	1440	400/200 (U/S)	-	66.3	4000/2000	7913	400/200 (U/S)	62.8	55.3	4000/2000
CE-GZSL [19]	63.3	43.1	7200	1440	100 (U)	70.4	70.0	24000	7913	2400 (U)	77.5	65.3	15000
FREE [17]	-	41.7	21600	1440	300 (U)	-	67.1	46000	7913	4600 (U)	-	57.7	35000
ICCE [21]	-	-	-	-	-	72.7	72.8	50000	7913	5000 (U)	78.4	66.4	20000
LCR-GAN [47]	-	49.8	43200	1440	600 (U)	-	-	-	-	-	59.7	20000	2967
RE-GZSL [20]	-	-	-	-	-	73.1	73.8	50000	7913	5000 (U)	78.9	67.0	20000
DENet [51]	-	45.8	7200	1440	100 (U)	-	72.0	35000	7913	3500 (U)	-	68.3	10000
DPCN [52]	63.8	43.3	5760	1440	80 (U)	70.6	71.4	25000	7913	2500 (U)	80.1	69.0	15000
Zheng et al. [53]	-	-	-	-	-	-	68.2	24000	7913	2400 (U)	-	68.3	35000
FSIGenZ (Ours)	67.8	45.9	1080	1440	15 (U)	75.0	74.2	900	7913	90 (U)	73.0	69.1	500
													10 (U)

Table 3: The ablation study of the proposed method with (w.) and without (w/o) DPSR and MSAS. The best and second-best results are highlighted in red and blue, respectively.

Method	SUN				AwA2				CUB			
	T1	U	S	H	T1	U	S	H	T1	U	S	H
Ours w/o MSAS w. DPSR	64.6	36.3	46.3	40.7	75.4	64.9	82.4	72.6	73.4	63.3	71.2	67.0
Ours w. MSAS w/o DPSR	65.3	12.0	46.0	19.1	69.7	8.8	93.3	16.1	46.9	16.2	59.5	25.5
Ours w/o MSAS w/o DPSR	64.5	12.5	45.1	19.6	72.0	11.0	95.8	19.8	62.8	20.6	54.0	29.9
Ours w. MSAS w. DPSR	67.8	42.5	49.9	45.9	75.0	67.6	82.3	74.2	73.0	65.9	72.7	69.1

for activation in the MLP, while ReLU and sigmoid functions are used in the contrastive network. The hyperparameter β is adjusted empirically (see sensitivity analysis).

4.2 Comparison With State-of-the-Art Methods

Table 1 presents a comprehensive comparison of recent methods on ZSL tasks for the SUN, AwA2, and CUB datasets. Specifically, FSIGenZ achieves the highest CZSL accuracy on SUN (67.8%) and AwA2 (75.0%), and also delivers competitive accuracy on CUB (73.0%). In the GZSL setting, it achieves harmonic mean (H) scores of 74.2% (AwA2), 69.1% (CUB), and 45.9% (SUN)—ranking as the best, second-best, and third-best method on these datasets, respectively. This level of consistent high performance across all datasets is unmatched by any other method in the table, many of which show strong results only in specific domains. Furthermore, methods that outperform FSIGenZ in GZSL on individual datasets—such as LCR-GAN (49.8%) and Vit-ZSL (49.3%) on SUN, and Vit-ZSL (71.0%) on CUB—do not report CZSL performance, making it difficult to assess their overall effectiveness. Taken together, FSIGenZ stands out as the most consistently effective method in Table 1, considering ZSL performance across all benchmarks.

Compared to other generative-based methods, FSIGenZ achieves the best CZSL Top-1 accuracy on SUN (67.8%) and AwA2 (75.0%), as well as the best GZSL harmonic mean on AwA2 (74.2%) and CUB (69.1%), while securing the second-best harmonic mean on SUN (45.9%), just behind LCR-GAN (49.8%). However, despite LCR-GAN’s higher harmonic mean on SUN, it falls short of FSIGenZ in CZSL Top-1 accuracy—indicating a weaker performance on the primary ZSL objective. A similar trend is observed on CUB, where DPCN records the highest CZSL accuracy (80.1%), but FSIGenZ surpasses it in harmonic mean (69.1% vs. 69.0%). Moreover, FSIGenZ requires only 15, 90, and 10 synthetic features per class, amounting to 1080, 900, and 500 total synthetic features for SUN, AwA2, and CUB respectively—orders of magnitude fewer than other generative models, which often synthesize thousands of features (see Table 2). For instance, LCR-GAN and DPCN synthesize up to 43200 and 15000 total unseen features on SUN and CUB respectively. Despite this, FSIGenZ outperforms or matches these methods in ZSL performance. This efficiency highlights a paradigm shift: instead of reframing ZSL as a fully supervised learning problem, FSIGenZ treats it more like a FSL problem by generating only a handful of informative synthetic features that capture the essential structure of unseen classes.

4.3 Ablation and Sensitivity Analysis

Ablation Study. In this section, we evaluate the impact of different components of the proposed method. We systematically remove various components—namely, MSAS and DPSR unit—from our method (see Table 3). Our full

model (last row), which integrates both MSAS and DPSR, achieves the best overall performance across all datasets. With DPSR removed, we observe a significant drop in GZSL performance, which indicates that the DPSR is crucial for generalization. Removing MSAS while retaining the DPSR leads to a more balanced performance across both CZSL and GZSL tasks, highlighting the DPSR’s role in maintaining prediction consistency. However, when both components are removed, the model’s performance declines significantly across all datasets, which confirms that both MSAS and the DPSR are essential for achieving high accuracy and generalization.

Impact of synthesized instances and β . We test the impact of varying the number of synthesized instances per unseen class to understand how this factor influences the model’s ability to generalize across different datasets. As shown in Fig. 5 (a-c), increasing the number of these instances affects the model’s performance and generalization capabilities and provides valuable insights into the optimal balance needed to achieve robust performance. In addition, we analyze the effect of β on model performance for each dataset (see Fig. 6 (a-c)). The results indicate that our method achieves optimal performance on all the datasets with β set to 0.2.

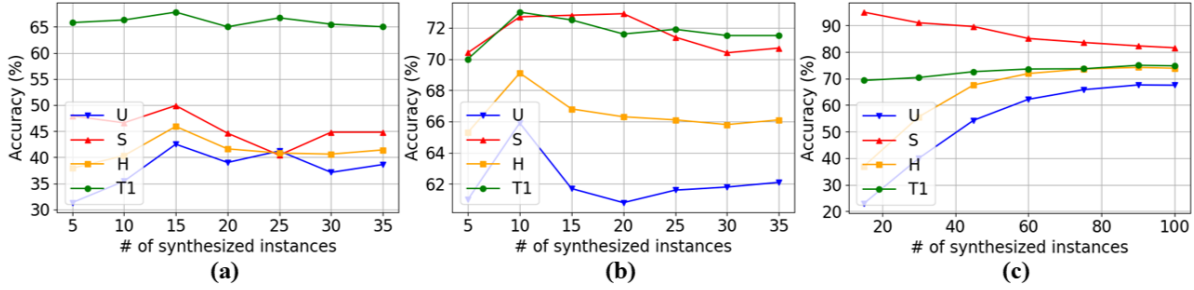


Figure 5: Results concerning varying synthetic instances for each unseen class of the (a) SUN, (b) CUB, and (c) AwA2 datasets.

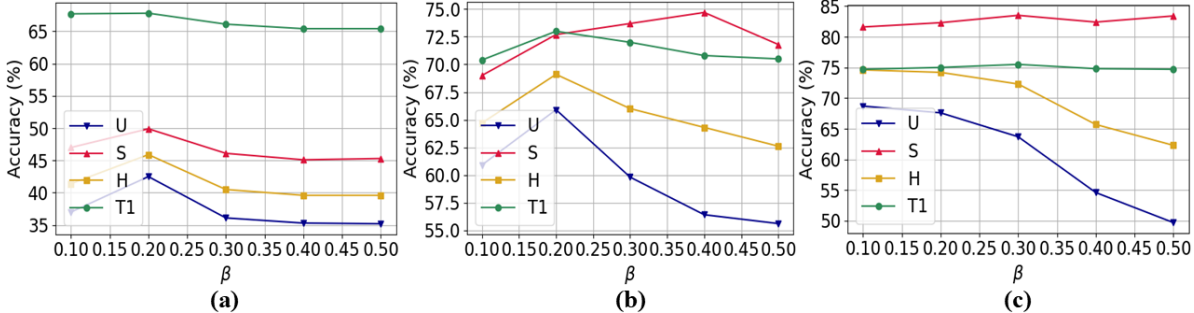


Figure 6: Results for various β values on (a) SUN, (b) CUB, and (c) AwA2 datasets.

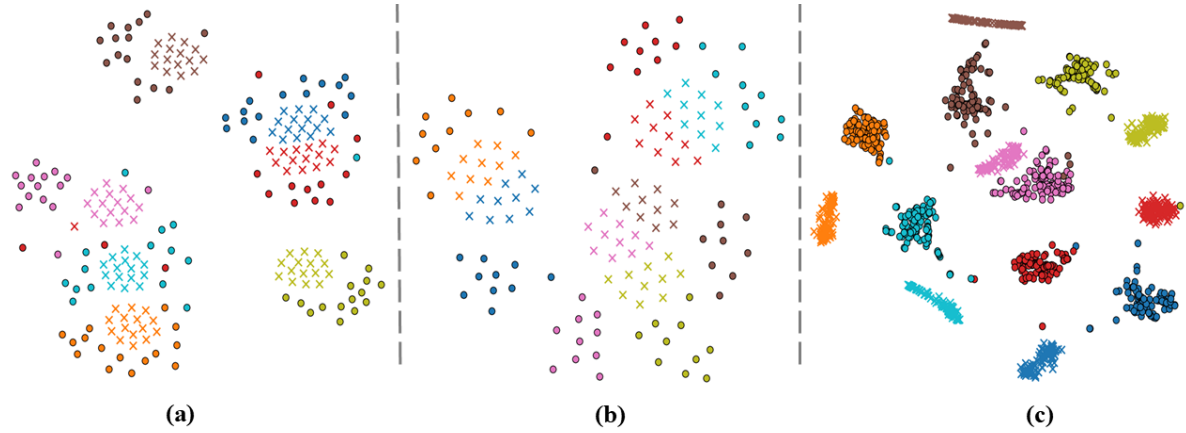


Figure 7: t-SNE visualization of seven randomly selected real (circle) and estimated (cross) clusters of the (a) SUN, (b) CUB and (c) AwA2 datasets.

Visualizing Subgroups in Unseen Class Space. To assess how well the synthesized prototypes represent the internal structure of unseen classes, we visualize real and estimated subgroup centroids using t-SNE on all three datasets (Fig. 7). Real sub-clusters (colored circles) are obtained via k-means on image features, while estimated prototypes (colored crosses) are generated by FSIGenZ. On SUN, despite its high intra-class variability, estimated prototypes align well with real clusters. In CUB, alignment remains strong despite its fine-grained nature. On AwA2, the match is especially close, reflecting its coarse-grained structure and strong attribute signals. These results highlight FSIGenZ’s ability to infer meaningful semantic subgroups using only class-level attributes.

5 Conclusion

In this paper, we present FSIGenZ, a unified zero-shot learning framework that combines feature generation and contrastive classification into a cohesive system. FSIGenZ synthesizes a compact set of semantically diverse subgroup prototypes per unseen class to avoid large-scale data generation. By modeling instance-level attribute variability, it estimates these prototypes and uses them as training data. To address class imbalance, a semantic regularization strategy is incorporated during the training of a contrastive classifier. FSIGenZ achieves competitive performance on SUN, CUB, and AwA2 datasets with significantly fewer synthetic features. By adopting a few-shot-inspired perspective, FSIGenZ reduces computational overhead and better preserves the original spirit of ZSL. In our future work, we will explore adaptive subgroup modeling to enhance performance in fine-grained domains.

References

- [1] Yongqin Xian, Christoph H Lampert, Bernt Schiele, and Zeynep Akata. Zero-shot learning—a comprehensive evaluation of the good, the bad and the ugly. *IEEE Trans. Pattern Anal. Mach. Intell.*, 41(9):2251–2265, 2018.
- [2] Christoph H Lampert, Hannes Nickisch, and Stefan Harmeling. Attribute-based classification for zero-shot visual object categorization. *IEEE Trans. Pattern Anal. Mach. Intell.*, 36(3):453–465, 2013.
- [3] Farhad Pourpanah, Moloud Abdar, Yuxuan Luo, Xinlei Zhou, Ran Wang, Chee Peng Lim, Xi-Zhao Wang, and QM Jonathan Wu. A review of generalized zero-shot learning methods. *IEEE Trans. Pattern Anal. Mach. Intell.*, 45(4):4051–4070, 2022.
- [4] Zhuo Chen, Yufeng Huang, Jiaoyan Chen, Yuxia Geng, Wen Zhang, Yin Fang, Jeff Z Pan, and Huajun Chen. Duet: Cross-modal semantic grounding for contrastive zero-shot learning. In *Proc. AAAI Conf. Artif. Intell.*, volume 37, pages 405–413, 2023.
- [5] Ian Goodfellow, Jean Pouget-Abadie, Mehdi Mirza, Bing Xu, David Warde-Farley, Sherjil Ozair, Aaron Courville, and Yoshua Bengio. Generative adversarial networks. *Commun. ACM*, 63(11):139–144, 2020.
- [6] Diederik P Kingma and Max Welling. Auto-encoding variational bayes. *arXiv preprint arXiv:1312.6114*, 2013.
- [7] Yongqin Xian, Tobias Lorenz, Bernt Schiele, and Zeynep Akata. Feature generating networks for zero-shot learning. In *Proc. IEEE Conf. Comput. Vis. Pattern Recognit.*, pages 5542–5551, 2018.
- [8] Shreyank N Gowda. Synthetic sample selection for generalized zero-shot learning. In *Proc. IEEE/CVF Conf. Comput. Vis. Pattern Recognit.*, pages 58–67, 2023.
- [9] Genevieve Patterson and James Hays. Sun attribute database: Discovering, annotating, and recognizing scene attributes. In *Proc. IEEE Conf. Comput. Vis. Pattern Recognit.*, pages 2751–2758. IEEE, 2012.
- [10] Catherine Wah, Steve Branson, Peter Welinder, Pietro Perona, and Serge Belongie. The caltech-ucsd birds-200-2011 dataset, 2011.
- [11] Yashas Annadani and Soma Biswas. Preserving semantic relations for zero-shot learning. In *Proc. IEEE Conf. Comput. Vis. Pattern Recognit.*, pages 7603–7612, 2018.
- [12] Yuxia Geng, Jiaoyan Chen, Zhiqian Ye, Zonggang Yuan, Wei Zhang, and Huajun Chen. Explainable zero-shot learning via attentive graph convolutional network and knowledge graphs. *Semant. Web*, 12(5):741–765, 2021.
- [13] Yang Liu, Xinbo Gao, Quanxue Gao, Jungong Han, and Ling Shao. Label-activating framework for zero-shot learning. *Neural Netw.*, 121:1–9, 2020.
- [14] Fei Zhang and Guangming Shi. Co-representation network for generalized zero-shot learning. In *Proc. Int. Conf. Mach. Learn.*, pages 7434–7443. PMLR, 2019.
- [15] Ziming Zhang and Venkatesh Saligrama. Zero-shot learning via semantic similarity embedding. In *Proc. IEEE/CVF Int. Conf. Comput. Vis.*, pages 4166–4174, 2015.

[16] Yongqin Xian, Saurabh Sharma, Bernt Schiele, and Zeynep Akata. f-vaegan-d2: A feature generating framework for any-shot learning. In *Proc. IEEE/CVF Conf. Comput. Vis. Pattern Recognit.*, pages 10275–10284, 2019.

[17] Shiming Chen, Wenjie Wang, Beihao Xia, Qinmu Peng, Xinge You, Feng Zheng, and Ling Shao. Free: Feature refinement for generalized zero-shot learning. In *Proc. IEEE/CVF Int. Conf. Comput. Vis.*, pages 122–131, 2021.

[18] Jiacheng Ye, Jiahui Gao, Qintong Li, Hang Xu, Jiangtao Feng, Zhiyong Wu, Tao Yu, and Lingpeng Kong. Zerogen: Efficient zero-shot learning via dataset generation. *arXiv preprint arXiv:2202.07922*, 2022.

[19] Zongyan Han, Zhenyong Fu, Shuo Chen, and Jian Yang. Contrastive embedding for generalized zero-shot learning. In *Proc. IEEE/CVF Conf. Comput. Vis. Pattern Recognit.*, pages 2371–2381, 2021.

[20] Yao Wu, Xia Kong, Yuan Xie, and Yanyun Qu. Re-gzsl: Relation extrapolation for generalized zero-shot learning. *IEEE Trans. Circuits Syst. Video Technol.*, 2024.

[21] Xia Kong, Zuodong Gao, Xiaofan Li, Ming Hong, Jun Liu, Chengjie Wang, Yuan Xie, and Yanyun Qu. En-compactness: Self-distillation embedding & contrastive generation for generalized zero-shot learning. In *Proc. IEEE/CVF Conf. Comput. Vis. Pattern Recognit.*, pages 9306–9315, 2022.

[22] Wenzhong Guo, Jianwen Wang, and Shiping Wang. Deep multimodal representation learning: A survey. *Ieee Access*, 7:63373–63394, 2019.

[23] Ali Jahanian, Lucy Chai, and Phillip Isola. On the "steerability" of generative adversarial networks. *arXiv preprint arXiv:1907.07171*, 2019.

[24] Yaogong Feng, Xiaowen Huang, Pengbo Yang, Jian Yu, and Jitao Sang. Non-generative generalized zero-shot learning via task-correlated disentanglement and controllable samples synthesis. In *Proc. IEEE/CVF Conf. Comput. Vis. Pattern Recognit.*, pages 9346–9355, 2022.

[25] Jacopo Cavazza, Vittorio Murino, and Alessio Del Bue. No adversaries to zero-shot learning: Distilling an ensemble of gaussian feature generators. *IEEE Trans. Pattern Anal. Mach. Intell.*, 2023.

[26] Dat Huynh and Ehsan Elhamifar. Compositional zero-shot learning via fine-grained dense feature composition. In *Adv. Neural Inf. Process. Syst.*, volume 33, pages 19849–19860, 2020.

[27] Jiang Lu, Jin Li, Ziang Yan, Fenghua Mei, and Changshui Zhang. Attribute-based synthetic network (abs-net): Learning more from pseudo feature representations. *Pattern Recognit.*, 80:129–142, 2018.

[28] Jiechao Guan, Zhiwu Lu, Tao Xiang, Aoxue Li, An Zhao, and Ji-Rong Wen. Zero and few shot learning with semantic feature synthesis and competitive learning. *IEEE Trans. Pattern Anal. Mach. Intell.*, 43(7):2510–2523, 2020.

[29] Yu-Ying Chou, Hsuan-Tien Lin, and Tyng-Luh Liu. Adaptive and generative zero-shot learning. In *Int. Conf. Learn. Represent.*, 2021.

[30] Bo Zhao, Botong Wu, Tianfu Wu, and Yizhou Wang. Zero-shot learning posed as a missing data problem. In *Proc. IEEE Int. Conf. Comput. Vis. Workshops*, pages 2616–2622, 2017.

[31] Dat Huynh and Ehsan Elhamifar. Fine-grained generalized zero-shot learning via dense attribute-based attention. In *Proc. IEEE/CVF Conf. Comput. Vis. Pattern Recognit.*, pages 4483–4493, 2020.

[32] Wenjia Xu, Yongqin Xian, Jiuniu Wang, Bernt Schiele, and Zeynep Akata. Attribute prototype network for zero-shot learning. In *Adv. Neural Inf. Process. Syst.*, volume 33, pages 21969–21980, 2020.

[33] Yizhe Zhu, Jianwen Xie, Zhiqiang Tang, Xi Peng, and Ahmed Elgammal. Semantic-guided multi-attention localization for zero-shot learning. In *Adv. Neural Inf. Process. Syst.*, volume 32, 2019.

[34] Huajie Jiang, Ruiping Wang, Shiguang Shan, and Xilin Chen. Transferable contrastive network for generalized zero-shot learning. In *Proc. IEEE/CVF Int. Conf. Comput. Vis.*, pages 9765–9774, 2019.

[35] Faisal Alamri and Anjan Dutta. Multi-head self-attention via vision transformer for zero-shot learning. *arXiv preprint arXiv:2108.00045*, 2021.

[36] Shiming Chen, Ziming Hong, Guo-Sen Xie, Wenhan Yang, Qinmu Peng, Kai Wang, Jian Zhao, and Xinge You. Msdn: Mutually semantic distillation network for zero-shot learning. In *Proc. IEEE/CVF Conf. Comput. Vis. Pattern Recognit.*, pages 7612–7621, 2022.

[37] Zhong Ji, Xuejie Yu, Yunlong Yu, Yanwei Pang, and Zhongfei Zhang. Semantic-guided class-imbalance learning model for zero-shot image classification. *IEEE Trans. Cybern.*, 52(7):6543–6554, 2022.

[38] Yun Li, Zhe Liu, Xiaojun Chang, Julian McAuley, and Lina Yao. Diversity-boosted generalization-specialization balancing for zero-shot learning. *IEEE Trans. Multimedia*, 25:8372–8382, 2023.

[39] Yuanyuan Yi, Guolei Zeng, Bocheng Ren, Laurence T Yang, Bin Chai, and Yuxin Li. Prototype rectification for zero-shot learning. *Pattern Recognit.*, 156:110750, 2024.

[40] Zongyan Han, Zhenyong Fu, Shuo Chen, Le Hui, Guangyu Li, Jian Yang, and Chang Wen Chen. Zs-vat: Learning unbiased attribute knowledge for zero-shot recognition through visual attribute transformer. *IEEE Trans. Neural Netw. Learn. Syst.*, 36(4):7025–7036, 2025.

[41] Rohit Keshari, Richa Singh, and Mayank Vatsa. Generalized zero-shot learning via over-complete distribution. In *Proc. IEEE/CVF Conf. Comput. Vis. Pattern Recognit.*, pages 13300–13308, 2020.

[42] Sanath Narayan, Akshita Gupta, Fahad Shahbaz Khan, Cees GM Snoek, and Ling Shao. Latent embedding feedback and discriminative features for zero-shot classification. In *Proc. Eur. Conf. Comput. Vis.*, pages 479–495. Springer, 2020.

[43] Shiming Chen, Guosen Xie, Yang Liu, Qinmu Peng, Baigui Sun, Hao Li, Xinge You, and Ling Shao. Hsva: Hierarchical semantic-visual adaptation for zero-shot learning. In *Adv. Neural Inf. Process. Syst.*, volume 34, pages 16622–16634, 2021.

[44] Zhe Liu, Yun Li, Lina Yao, Xianzhi Wang, and Guodong Long. Task aligned generative meta-learning for zero-shot learning. In *Proc. AAAI Conf. Artif. Intell.*, volume 35, pages 8723–8731, 2021.

[45] Zhongqi Yue, Tan Wang, Qianru Sun, Xian-Sheng Hua, and Hanwang Zhang. Counterfactual zero-shot and open-set visual recognition. In *Proc. IEEE/CVF Conf. Comput. Vis. Pattern Recognit.*, pages 15404–15414, 2021.

[46] Junhan Kim, Kyuhong Shim, and Byonghyo Shim. Semantic feature extraction for generalized zero-shot learning. In *Proc. AAAI Conf. Artif. Intell.*, volume 36, pages 1166–1173, 2022.

[47] Yalan Ye, Tongjie Pan, Tonghoujun Luo, Jingjing Li, and Heng Tao Shen. Learning mlatent representations for generalized zero-shot learning. *IEEE Trans. Multimedia*, 25:2252–2265, 2023.

[48] Hongzu Su, Jingjing Li, Ke Lu, Lei Zhu, and Heng Tao Shen. Dual-aligned feature confusion alleviation for generalized zero-shot learning. *IEEE Trans. Circuits Syst. Video Technol.*, 33(8):3774–3785, 2023.

[49] Yang Liu, Yuhao Dang, Xinbo Gao, Jungong Han, and Ling Shao. Zero-shot learning with attentive region embedding and enhanced semantics. *IEEE Trans. Neural Netw. Learn. Syst.*, 35(3):4220–4231, 2024.

[50] Xiao Li, Min Fang, and Zhibo Zhai. Joint feature generation and open-set prototype learning for generalized zero-shot open-set classification. *Pattern Recognit.*, 147:110133, 2024.

[51] Jiannan Ge, Hongtao Xie, Pandeng Li, Lingxi Xie, Shaobo Min, and Yongdong Zhang. Towards discriminative feature generation for generalized zero-shot learning. *IEEE Trans. Multimedia*, 2024.

[52] Huajie Jiang, Zhengxian Li, Yongli Hu, Baocai Yin, Jian Yang, Anton van den Hengel, Ming-Hsuan Yang, and Yuankai Qi. Dual prototype contrastive network for generalized zero-shot learning. *IEEE Trans. Circuits Syst. Video Technol.*, 35(2):1111–1122, 2025.

[53] Baolong Zheng, Zhanshan Li, and Jingyao Li. Class-wise and instance-wise contrastive learning for zero-shot learning based on vaegan. *Expert Syst. Appl.*, page 126671, 2025.

[54] Alexey Dosovitskiy, Lucas Beyer, Alexander Kolesnikov, Dirk Weissenborn, Xiaohua Zhai, Thomas Unterthiner, Mostafa Dehghani, Matthias Minderer, Georg Heigold, Sylvain Gelly, Jakob Uszkoreit, and Neil Houlsby. An image is worth 16x16 words: Transformers for image recognition at scale. *arXiv preprint arXiv:2010.11929*, 2020.